.

# Quantum Gravity Unification Model with Fundamental Conservation

Arthur E. Pletcher[1]
[1]*International Society for Philosophical Enquiry, Winona, Minnesota, USA*

email: artpletcher@ultrahighiq.org 

**Abstract**

A fundamental conservation and symmetry is proposed, as a unification between General Relativity (GR) and Quantum Theory (QT). Unification is then demonstrated across multiple applications. First, as applied to cosmological redshift $z$ and energy density $\rho$. Then, a local system galaxy rotational curve is examined. Next, as applied to Quantum Mechanics' "time problem": Absolute and relative notions of time are shown to be reconcilable, as well as renormalization values between scales. Finally, as applied to the Cosmological Constant: The discrepancy that exists between the vacuum energy density in GR at critical density: $\rho_{cr} = 3H^2/8\pi G = 1.88(H^2)x10^{-29}g/cm^3$ [1], and the much greater zero-point energy delta value as calculated in quantum field theory (QFT) with a Planck scale ultraviolet cutoff: $\rho_{hep} = M^4c^3/h^3 = 2.44x10^{91}g/cm^3$ [2] is resolved to null orders of magnitude.

## 1. INTRODUCTION

Special relativity (SR) eloquently conforms to $\frac{Mv^2}{2}$ (total kinetic energy) in Noether's theorem as, [3]

$$E_k = \frac{Mc^2}{\sqrt{\frac{1-v^2}{c^2}}},$$

and energy is thus conserved (time-transitionally invariant). However in GR, energy evolves as spacetime changes. Einstein has shown us that when the space through which particles move is dynamic, the total energy of those particles is not conserved. Moreover, the energy stored in the cosmological constant must expand at a rate of $k^3$, in proportion to the volume of expanding space. An additional challenge to vacuum energy is the unstable nature of uneven distribution of matter throughout the universe. The pervading justification for red shift photon energy loss is the lack of an associated symmetry.

Conservation laws conventionally define invariance with respect to time. For example, the Euler-Lagrange equations (in general coordinates), [4]

$$\frac{d}{dt}\left(\frac{\partial L}{\partial \dot{q}}\right) = \frac{\partial L}{\partial q}$$

Then conservation is shown by the first order derivative of some quantity, with respect to time, being equal to zero,

$$\frac{d}{dt}\left(\frac{\partial L}{\partial \dot{q}_k}\right) = \frac{dp_k}{dt} = 0$$

**However, this article proposes a fundamental conservation of total Hamiltonian energy within the entire scope of cosmology.**

## 2. THE SUPERNOVA COSMOLOGY PROJECT WITH EINSTEIN-DE SITTER MODEL

The 1998 supernova data [5] have concluded that observed magnitude of nearby and distant type LA supernovae, as compared with cosmological predictions of models with zero vacuum energy and mass densities (ranging from the critical density $\rho_c$ down to zero), has formally ruled out the Einstein-de Sitter model of closed ordinary matter (i.e. $\Omega_M = 1$) at the $7\sigma$ to $8\sigma$ confidence level for two different fitting methods. Moreover, the best fit to this divergence implies that, in the present epoch, the vacuum energy density $\rho_\Lambda$ is larger than the energy density attributable to mass ($\rho_m C^2$). Therefore, the cosmic expansion is now accelerating. **However, an alternate interpretation of this data is presented,**

**in defiance of a requirement for any dark component of energy density:**

**Theorem 2.1** *Time interval $\Delta t$ contracts (decreases) inversely proportional to the metric expansion of space $ar$, independent of relative motion (Note that this is distinct from $\gamma$ time dilation).*

$$\frac{\Delta t_n}{\Delta t} = \frac{\Delta a r_0}{\Delta a r_n} = \frac{\Delta D_0}{\Delta D_n}$$

*Normalizing $\Delta t_n$ from $D$,*

$$\Delta t_n = \frac{1}{1 + DK}$$

*Where $\Delta t_n$ is an interval of time at distance $D_n$, and $K$ is an undetermined minute constant ($\approx 4.000E-24$) that becomes significant in a matter dominated universe.*

Thus, accelerating expansion is alternatively explained as being generally constant, such that $\ddot{a} = 0$ (excluding local variation) with a decrease in time interval $\Delta t_n$, which has an equivalent effect as an increase in velocity $v$. Thus,

**Corollary 2.1.1** *Universal expansion, with decreasing time intervals, appears as accelerated expansion.*

Note that this offers an alternative to dark components, as functions with decreasing time intervals are equivalent to functions with an anti-derivative. See figure 1

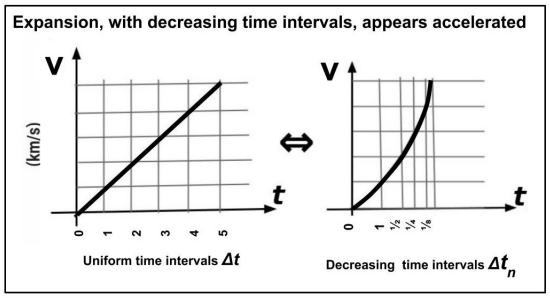


Figure 1: Velocity $\dot{a}(t)$ with decreasing time intervals appears as acceleration $\ddot{a}(t)$

Table I lists eleven hypothetical sla points as predicted in the Einstein-de Slitter model with uniform time intervals, compared with contracted time intervals ($\Delta t_n$, per theorem 2.1). The scatter plot in figure 2 (with logarithmic horizontal axis) shows three trend-lines with corresponding values of K $\approx (\Omega_M, \Omega_\Lambda) = (0,1), (0.5,0.5), (1,0)$. Note: $\ddot{a}(t) = 0$.

Table I: Predicted Einstein-de Slitter model with uniform time intervals, compared with contracted time intervals. In successive columns: $[m_b]$ (magnitude brightness), z (Redshift), $\Delta t_n$ $[K_a = 0]$, $\Delta t_n$ $[K_b$=2.000 x $10^{-24}]$, $\Delta t_n$ $[K_c$=4.000 x $10^{-24}]$

| $m_b$ | **z** | $\Delta t_n$ $[K_a]$ | $\Delta t_n$ $[K_b]$ | $\Delta t_n$ $[K_c]$ |
|---|---|---|---|---|
| 14 | 0.010 | 1.000 | 0.998 | 0.997 |
| 15 | 0.016 | 1.000 | 0.996 | 0.995 |
| 16 | 0.025 | 1.000 | 0.994 | 0.993 |
| 17 | 0.040 | 1.000 | 0.990 | 0.988 |
| 18 | 0.063 | 1.000 | 0.985 | 0.982 |
| 19 | 0.100 | 1.000 | 0.976 | 0.971 |
| 20 | 0.158 | 1.000 | 0.963 | 0.955 |
| 21 | 0.250 | 1.000 | 0.942 | 0.931 |
| 22 | 0.396 | 1.000 | 0.911 | 0.895 |
| 23 | 0.628 | 1.000 | 0.866 | 0.843 |
| 24 | 0.996 | 1.000 | 0.803 | 0.772 |

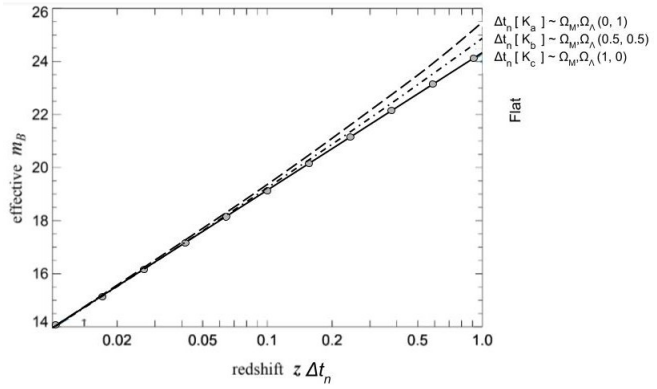


Figure 2: Hypothetical sla points as predicted in the Einstein-de Slitter model with uniform time intervals, compared with contracted time intervals

## 3. ENERGY DENSITY INCREASES WITH $\Delta t_n$

**Corollary 3.0.1** *Per theorem 2.1, velocity $\frac{\Delta d}{\Delta t_n}$ increases with distance $ar$. With this proportionate increase in velocity, energy density $\rho$ proportionally increases, due to increased velocities in particle kinetic and internal energies (compression, energy of nuclear binding, etc.). To the observer at $ar_0$, energy at $ar_n$ [mpc] density measures $\rho_n$ with greater energy per unit of time.*

$$\frac{\Delta \rho_n}{\Delta \rho} = \frac{\Delta t_n}{\Delta t}$$

### Conservation of Energy Density Over Flat Space

Einstein had contemplated that his original static model of GR was unstable, and might require the cosmo-

logical constant to offset gravity from collapsing. However, this alternate model is inherently more stable:

**Corollary 3.0.2** *For galactic scales, at distance $ar_n$, the average force of energy density $\rho$, approaching from below $ar_n$, is counterbalanced by the average force of increasing energy density $\rho_n$ approaching from above $ar_n$,*

$$\lim_{r\to -r_n} \frac{\partial \rho}{\partial (ar)} = \lim_{r\to +r_n} \frac{\partial \rho_n}{\partial (ar)}$$

Thus, a fundamental conservation and coordinate symmetry of energy density, with respect to spacetime, is established. See figure 3,

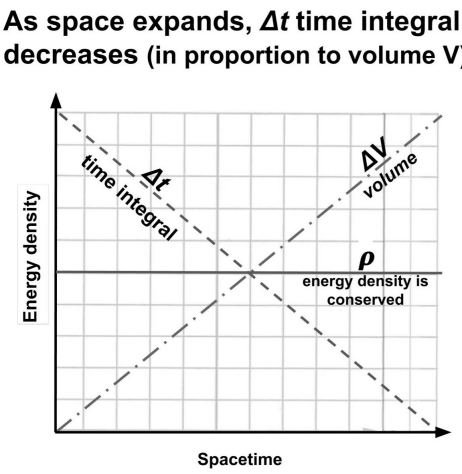


Figure 3: Fundamental conservation and coordinate symmetry of energy density, with respect to spacetime

### Galaxy Rotation Curve with Increased Density

The discrepancies between theoretical and observed galaxy rotation curves involve both density and velocity. Conventionally, the dependence of circular velocity $V_{circ}$ on radial distance $R$ assumes $M$, $m$ and velocity to be fixed over large scales in Kepler's law, [6]

$$T^2 = \frac{4\pi^2 r^3}{GM} \Rightarrow T^2 \propto r^3$$

Moreover, gravitational lensing demonstrates the existence of a much greater Mass (density) than the sum of the stars within the galaxy. **However, this alternate model specifically addresses these two issues and provides an explanation,**

**Corollary 3.0.3** *Per theorem 2.1 and corollary 3.0.1, velocity $\frac{\Delta d}{\Delta t_n}$ and density $\rho_n$ are measured with increased magnitude per distance $ar_n$. This directly extends to energy density within galaxies and the effects on rotational velocity, such that: As $R$ increases, centripetal force is perfectly balanced by increases in $v$ ($\frac{\Delta d}{\Delta t_n}$) and, subsequently, $\rho_n$,*

$$\frac{v^2}{r} = \frac{G}{r^2} M = \frac{G}{r^2} \int \rho_n dt$$

Note: total mass $M$ inside the circle of the radius $r$ can be obtained by doing integration of mass density in a volume. $M = \int \rho_n dt$ Note:

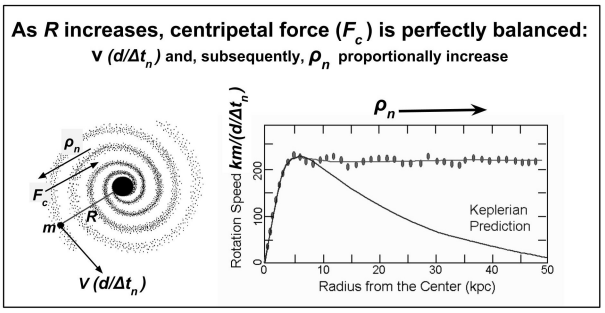


Figure 4: Flat galaxy rotation curve explained with fundamental conservation

- $\rho = \rho_R$ and $\rho_M$ (Dark components are excluded from this model, with the intent of presenting an alternative).
- Along with time dilation $\gamma$, time contraction $\Delta t_n$ is a distinct and necessary factor in deriving proper time
- $\Omega = 1$ (flat space)
- The expanding universe is homogeneous, isotropic and asymptotically flat.

## 4. QUANTUM MECHANICS TIME PROBLEM

Theorem 2.1 of time contracting inversely with space expansion can be restated in reverse:

**Theorem 4.1** *As scales approach Planck length, time intervals dilate (independent of their relative motion in SR) to a range, represented as an integral from $-t_n$past to $+t_n$ future. As well corresponding values of position, energy, density and charge become superimposed within this range.*

More concisely, this is presented as a unifying explanation of superposition. Figure 5 shows how both GR and QM are unified by this single basic premise. Viewed from classic scale (with projectile), the time intervals of orbits vary, as opposed to being fixed. The result is the integration of position, energy, density and charge.

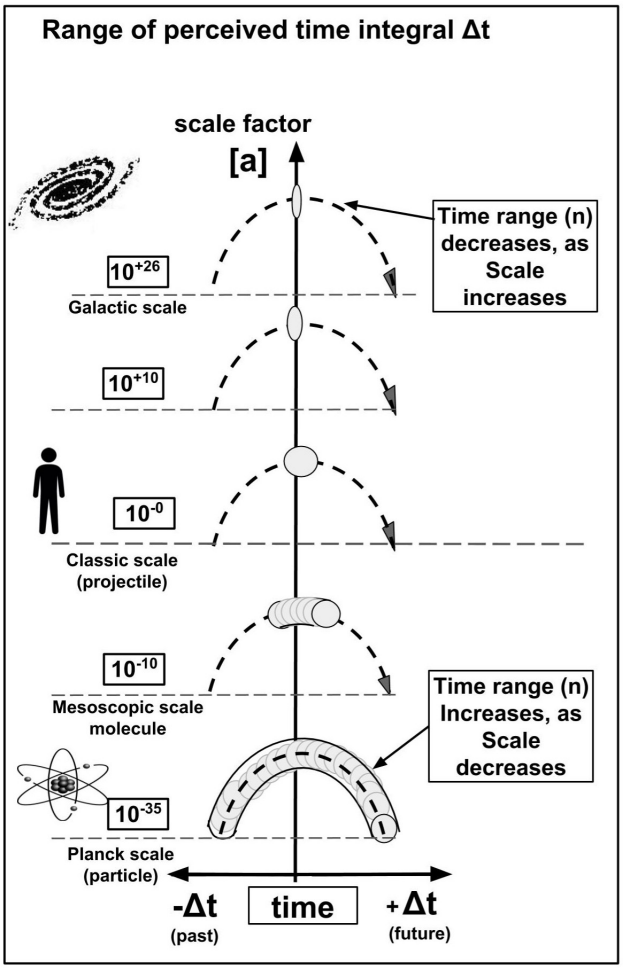


Figure 5: Gr and QM are unified

This assertion also challenges the use of mass in De-Broglie's $\lambda$ by substituting a unit of length (scale), such as $r_e$ (electron radius) or $r_0$ (atomic radius), instead of mass:

Hydrogen atom wave function (for plane wave): [7]

$$\Psi_{\vec{k}(\vec{r})} = e^{i\vec{k}\cdot\vec{r}} \tag{1}$$

Using $p = \hbar k$ for momentum, the dominate wave function $Psi_{\vec{k_0}}$ includes wave vector $\vec{k_0}$ :

$$k_0 = \frac{2\pi}{\lambda_0} \implies \lambda \propto -d \tag{2}$$

thus,

**Corollary 4.1.1** *wave length is inversely proportional to distance,*

$$\lambda \propto -d$$

Extending this relationship to superposition,

**Corollary 4.1.2** *From classic space, the observer notices an expanded range (superposition) of time, position, momentum and energy { t, x, p, e }. Essentially, observing an integral of past, present and future in a single instant, (conceptually, like a time-lapse image), appearing as a semi dense solid.*

So a particular orbit might appear as a torus. If the "range" is subatomic (< the orbit diameter) a projectile might appear as a partial torus. See figure 6

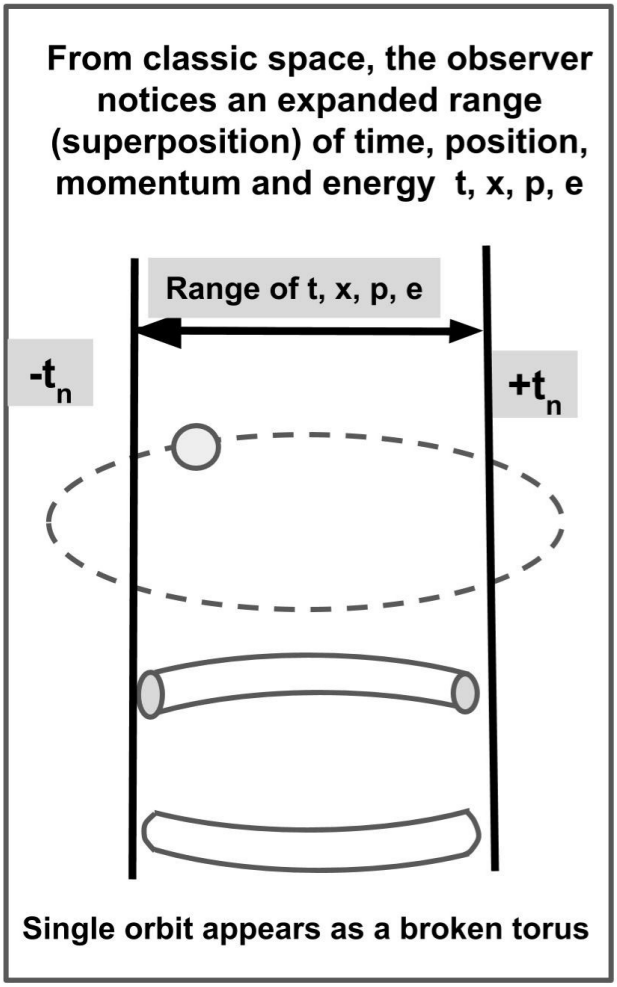


Figure 6: Orbitals with gaps

**Probability Density and complex functions**

Modeling superposition, in the time dependent wavefunction, as expanded time (with corresponding positions) sheds some light on the role of complex numbers in the wavefunction probability distribution, [8]

$$P\big(x_1 \le x \le x_2\big) = \int_{x_1}^{x_2} |\Psi|^2 dx$$

**If we may represent $\Psi$ as a function of position $x_{range}$ with an orthogonal of $\Delta t_{range}$ ($-n$ past to $n$ future), then this suggests a requirement of $2D$ planar values in complex numbers** See figure 7.

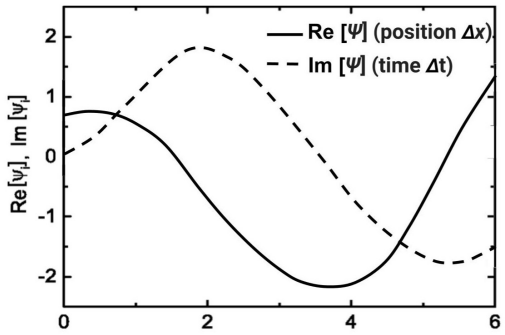


Figure 7: Real and imaginary numbers represent $\Delta t_{range}$ time and position $x_{range}$

Note: In this model, probability density (as captured by $\Psi(x)\Psi*(x)$ complex conjugate) represents a density range of both time and corresponding position. With this understanding and reference to the Bohr model, a higher probability density is expected toward the center, where orbiting paths are more frequent. Also note that this model easily explains orbital gaps as electron orbits outside of this range. See figure 8.

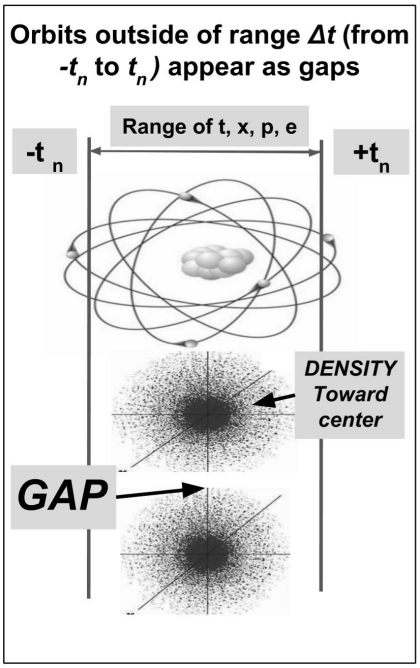


Figure 8: Gaps and density explained

## 5. COSMOLOGICAL CONSTANT $\Lambda$ ($\rho_{cos}$) IN GR

Per theorem 2.1, accelerating expansion is shown to be an illusion ($\ddot{a} = 0$). See figure 1. The rate of convergence corresponds to $\Delta t_n$. Thus cancelling the need for adding $\Lambda$ to Einstein's field equations. We are left with the original form of: [9]

$$R_{\mu\nu} - \frac{1}{2}Rg_{u\nu} = \frac{8 \times \pi G}{c^4}T_{\mu\nu} \tag{3}$$

## 6. VACUUM ENERGY DENSITY ($\rho_{hep}$) IN QM

Theorem 4.1 ("As scales approach Planck length, time intervals dilate to a range, represented as an integral from -$t_n$ past to +$t_n$ future. As well corresponding values of position, energy, density and charge become superimposed within this range".), and corollary 4.1.1 ("wave length is inversely proportional to distance") provides a reasonable alternative to the unreasonable sum of vacuum energy (even within a restricted cutoff of photon energy being equal to Planck energy):

**Corollary 6.0.1** *As measured from classic scale, the Casimir force (U) between plates a distance x micrometers apart represents a much greater range (n) of expanded time interval, along with associated values of position, energy, momentum and charge.* ***This range (n) increases as*** $x$ ***decreases.***

$$U_{range} = \int_{-t_n}^{t_n}\int_{-q_n}^{q_n}\frac{U}{\lambda}\,dt$$

Where (q) is general positional coordinates. Thus, the assumed force measured in a unit of volume is instead a much greater integral over, both time (-$t_n$ past to +$t_n$ future) and position (-$q_n$ to $q_n$). Note that as $\lambda$ decreases $U$ increases (See figure 9,

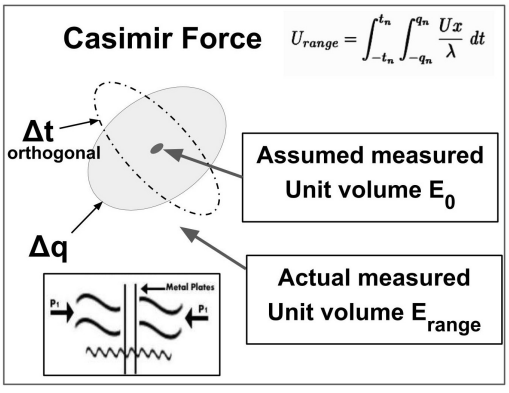


Figure 9: Casimir force energy U represents an integral (range) of both time and position

## 7. SUPPORTIVE EVIDENCE

### Apparent Deviation From Kepler's Orbital Laws

Theorem 2.1, is supported by the following correlation study: "On Possible Systematic Redshifts Across the Disks of Galaxies" [10]. This study shows a deviation from Kepler's orbital laws, specifically on the subject of increased velocity on the far sides of multiple galaxies. Although not conclusive, it does justify consideration to this article.

Note that multiple galaxy surveys with increased velocities across their minor axis. Thus, **velocity within the same body appears to increase per distance.** "Velocity observations in 25 galaxies have been examined for possible systematic redshifts across their disks: a possible origin for the redshifts could be the radiation fields. Velocities increase towards the far sides in most cases. This is so for the ionized gas, for neutral hydrogen, and in some cases for the stars. The effect is seen as velocity gradients along the minor axes, as well as in velocity fields of neutral hydrogen in other parts of the galaxies. Deviation of the kinematic major axis from the optical axis is found for 10 galaxies and in 9 of these the largest velocities occur in the far side. In the central regions of four galaxies are found large velocity gradients in the same direction. While expanding motions provide an explanation for some of these features, it remains difficult to thereby explain all the peculiarities found. Faintness of the data available in this preliminary study should be noticed. Observations specially programmed for this subject would be necessary."

Figure 10 shows 'table 1', on page 258 which lists 25 galaxies, correlation coefficients and relevant columns (including sources of data):

258 T. Jaakkola *et al.*

Table 1. List of galaxies for which velocities along the minor axis are available. In successive columns: type; distance; angle between rotation axis of galaxy and line of sight; regression and correlation coefficients between velocity and distance; source of data

| NGC | Type | $d$ (Mpc) | $i$ | $h$(kms$^{-1}$kpc$^{-1}$) | $\varrho$ | Source of data |
|---|---|---|---|---|---|---|
| 224 | Sb | 0.69 | 77° | 0.20 | 0.272 | Gottesman and Davies (1970) |
| 253 | Sc | 4.0 | 78 | 0.13 | 0.012 | Burbidge *et al.* (1963a) |
| 300 | Sd | 2.4 | 43 | 1.03 | 0.844 | Shobbrook and Robinson (1967) |
| 598 | Scd | 0.72 | 57 | 1.51 | 0.866 | Gordon (1971) |
| 613 | SBbc | 15 | 47 | 57.09 | 0.820 | Burbidge *et al.* (1964c) |
| 972 | SBc | 17 | 66 | −11.31 | −0.670 | Burbidge *et al.* (1965) |
| 1084 | Sc | 14 | 65 | − 4.75 | −0.338 | Burbidge *et al.* (1963b) |
| 1097 | SBb | 12 | 50 | 5.00 | 0.105 | Burbidge and Burbidge (1960) |
| 1365 | SBb | 15 | 66 | −79.21 | −0.976 | Burbidge *et al.* (1962a) |
| 1792 | Sbc | 10 | 64 | 10.12 | 0.587 | Rubin *et al.* (1964) |
| 2403 | Scd | 3.3 | 55 | 0.04 | 0.118 | Burns and Morton (1971) |
| 3310 | Sbc | 11 | 31 | 61.27 | 0.815 | Walker and Chincarini (1967) |
| 3521 | Sbc | 7.6 | 66 | 7.18 | 0.056 | Burbidge *et al.* (1964b) |
| 4736 | Sab | 3.3 | 40 | 44.28 | 0.849 | Chincarini and Walker (1967) |
| 4826 | Sab | 7.3 | 60 | 39.16 | 0.854 | Rubin *et al.* (1965) |
| 5194 | Sbc | 4.0 | 35 | −15.18 | −0.758 | Burbidge *et al.* (1964a) |
| 5248 | Sbc | 11 | 55 | −26.94 | −0.690 | Burbidge *et al.* (1962b) |
| 5457 | Scd | 3.5 | 27 | − 1.40 | −0.403 | Rogstad and Shostak (1971) |
| 6574 | Sbc | 33 | 45 | 4.73 | 0.428 | Demoulin and Tung Chan (1969) |
| 7469 | Sa | 51 | 49 | 8.69 | 0.552 | Burbidge *et al.* (1963c) |

Figure 10: two vectors, observed at $d = 1mpc$, with different radial velocities

### Prediction as Supportive Evidence

One prediction of decreasing time intervals would be: Galaxies with a negative $z$ value (approaching instead of receding, in our local group) would also correlate with distance, such that the furthest galaxies would appear to approach with the fastest velocity.

## 8. CONCLUSIONS

In order to define the fundamental conservation and symmetry of spacetime, within the broad scope of cosmology, it is necessary to consider some independent parameter representing constant energy. Once this conservation is established, simple and parsimonious resolution to applications in General Relativity, Quantum Mechanics and the Cosmological constant become both plausible and reasonable.

[1] R. L. Oldershaw. Self-similar cosmological model: Introduction and empirical tests. *International Journal of Theoretical Physics*, 1989.
[2] S. M. Carol. The cosmological constant. *Annual review of astronomy and astrophysics, Vol 30*, 1992.
[3] R. Brehme. *Introduction to the Theory of Relativity*. Addison-Wesley Series in Physics, 1968.
[4] M Hazewinkel. *Lagrange equations (in mechanics)*. Kluwer Academic Publishers, 2001.
[5] S. Perlmutter. Measurements of omega and lambda from 42 high-redshift supernovae. *arXiv.org*, 1998.
[6] E. Butikov. Motions of celestial bodies. *IOP Publishing*, 2014.
[7] I. R. Afnan. *Quantum Mechanics with Applications*. Bentham Science Publishers, 2010.
[8] N.G. Ushakov. *Density of a probability distribution / Encyclopedia of Mathematics*. Springer, 2001.
[9] S. Weinberg. *Gravitation and Cosmology*. John Wiley Sons, 1972.
[10] T. Jaakkola, P. Teerikorpi, and K. Donner. On possible systematic redshift across the disks of galaxies. *Astronomy and Astrophysics.*, 1975.